ISSN (Print) : 0974-6846
ISSN (Online) : 0974-5645
Indian Journal of Science and Technology, *Vol 11(1), DOI: 10.17485/ijst/2018/v11i1/116538, January 2018*

Investigation of Sinusoidal Phase Voltage Effect on SFR Calculation of HVAC Transmission Lines

Nima Bababaglou[1*], Behrooz Vahidi[1], Abolfazl Rahiminejad[2]

[1]Department of Electrical Engineering, Amirkabir University of Technology, Iran;
n.bababagloo@aut.ac.ir, vahidi@aut.ac.ir
[2]Department of Electrical and Computer Science, Esfarayen University of Technology,
arahiminezhad@aut.ac.ir

Abstract

Objectives: In this paper, the conductor's voltage effects on shielding failure calculation of high voltage transmission lines are investigated. A new criterion for distinguishing the stable upward leader formation is also proposed. **Methods/ Statistical Analysis:** Charge simulation method is used for modeling of the 3-D stepwise movement of lightning downward leader. For determination of striking point and Shielding Failure (SF) calculation, a new criterion for distinguishing the stable upward corona-leader system formation is proposed. The proposed criterion is developed in a way that the effects of operating voltage including the magnitude, phase and the sign of voltage are considered in the stable upward leader formation. **Findings**: The results of the simulated lightning, using the proposed criterion show that the proposed model simulates the lightning stroke phenomenon close to reality. The amount of the required electric field for stable upward leader inception from the phase wires with various voltage levels and signs, are calculated by proposed criterion. The results, in line with field experiments, revealed that the probabilities of upward leader inception and also lightning strokes change with variation of operating voltage of conductors. In the conductors with positive voltage, the required electric field for upward leader inception is far lower than the conductors with zero or negative voltage. Moreover the SF of a 500KV-HVAC transmission line is obtained and compared in two cases i.e., with consideration and without consideration of voltage effects. The result showed that SFR and maximum return stroke current increase 19% and 14%, respectively, by consideration of phase voltage effects. Which means voltage has great effects on SF calculation and should not be neglected. **Novelty/Improvements:** The proposed method improved SF Calculation by 1-Considering the effects of operating voltage including the magnitude, phase and sign of voltage2-Accurate modeling of downward leader and its charge in space.

Keywords: Lightning, Leader Progression Model, Shielding Failure Calculation, Sinusoidal Voltage of HVAC Transmission Line

1. Introduction

High voltage transmission lines, as a vital part of power systems in transferring electricity power to end users, is exposed to variety of natural threats such as lightning[1]. Direct lightning strokes to the phase wires which refers to Shielding Failure (SF), is a main reason of power system interruptions. Since, appropriate allocation of shield wires, which needs to high accurate calculation of SF, is a key factor in high voltage transmission lines designing. Electro geometric Model (EGM) is the most popular

*Author for correspondence

method for SF calculation, which is first, introduced[2] and expanded by the some other researchers[3–9]. However, the comparisons of field observations with the results of this method, reveals that the accuracy of the method may not be very acceptable[10]. Therefore, a new method known as Leader Progression Model (LPM), which is based on the physical phenomena of lightning expansion through the air, was introduced[10,11] and was used widely by many researchers[12–15].

The more accurate the striking point is determined, the more accurate the SF is calculated. Identification of stable upward leader inception which is distinguished by different criteria is a main factor for SF calculation using LPM. In a majority of articles such as[12–16], the effect of phase voltage is not taken into consideration in stable upward leader formation. In other words, the upward leader incepted from the phase wire is the same with that from a conductor with zero voltage level. This shortcoming is also existing in the improved LPM of[15], in which the effect of voltage is just considered in the critical current (I_c).

In this paper, Shielding Failure (SF) of high voltage transmission lines is calculated considering phase wire sinusoidal voltage effects. The 3-D LPM is used for modeling of the negative lightning downward leader propagation based on its physical characteristics. Unlike the conventional LPM model in which only the downward leader channel is modeled, in this paper, corona sheath and space charges associated with leader movement are considered. The lightning striking point is determined based on a new developed criterion for stable upward corona-leader system identification. The mentioned criterion is developed, in this paper, in a way that the effects of operating voltage including the magnitude, phase and the sign of voltage (i.e., the sinusoidal nature of voltage), are considered in the stable upward leader formation. The space of study including the cloud, towers, and conductors with their sag are modeled using CSM. Finally, the SF of 500kV-HVAC transmission lines is calculated in two cases i.e., with consideration and without consideration of the voltage effect, and the results are discussed. Moreover, the results of this paper are compared to those of other researchers, which are based on electromagnetic and electro geometric methods, and field observations and discussed.

2. Lightning Downward Leader Modeling

Lightning downward leader modeling includes the model of leader main channel and its charge distribution, charge around the corona sheath, and downward leader direction.

Based on the actual observations of downward leader of lightning, the leader approaches the earth stepwise. In other words, downward leader goes down toward to earth in halting steps. After each step, the leader stops, then moves along one or more paths. The length of each step is in the range of 10 to 100 meters[17]. The length of the steps depends on the height of leader tip. The average length of the steps is 100 meter near the cloud; while, it decreases to roughly 10 meter near the ground[17].

In this paper, charge simulation method is used for electric fields and electrical potential calculation. In this method, all parts simulated by point charges, line charges and ring charges, which are replaced with actual charges[18,19]. For the modeling of downward leader channel and its stepping propagation, line charges with vertical/horizontal sections are used. As it seen in Figure 1 downward leader modeling is started by a vertical line charge with the length of 500m. Based on[14], for the next step direction, a hemisphere with the radius of the next step length (i.e., 1/5 of height of leader tip) and the center of the leader tip is drawn. Since the negative downward leader is considered in this paper, the next jump point of the leader is a point on the hemisphere where the absolute

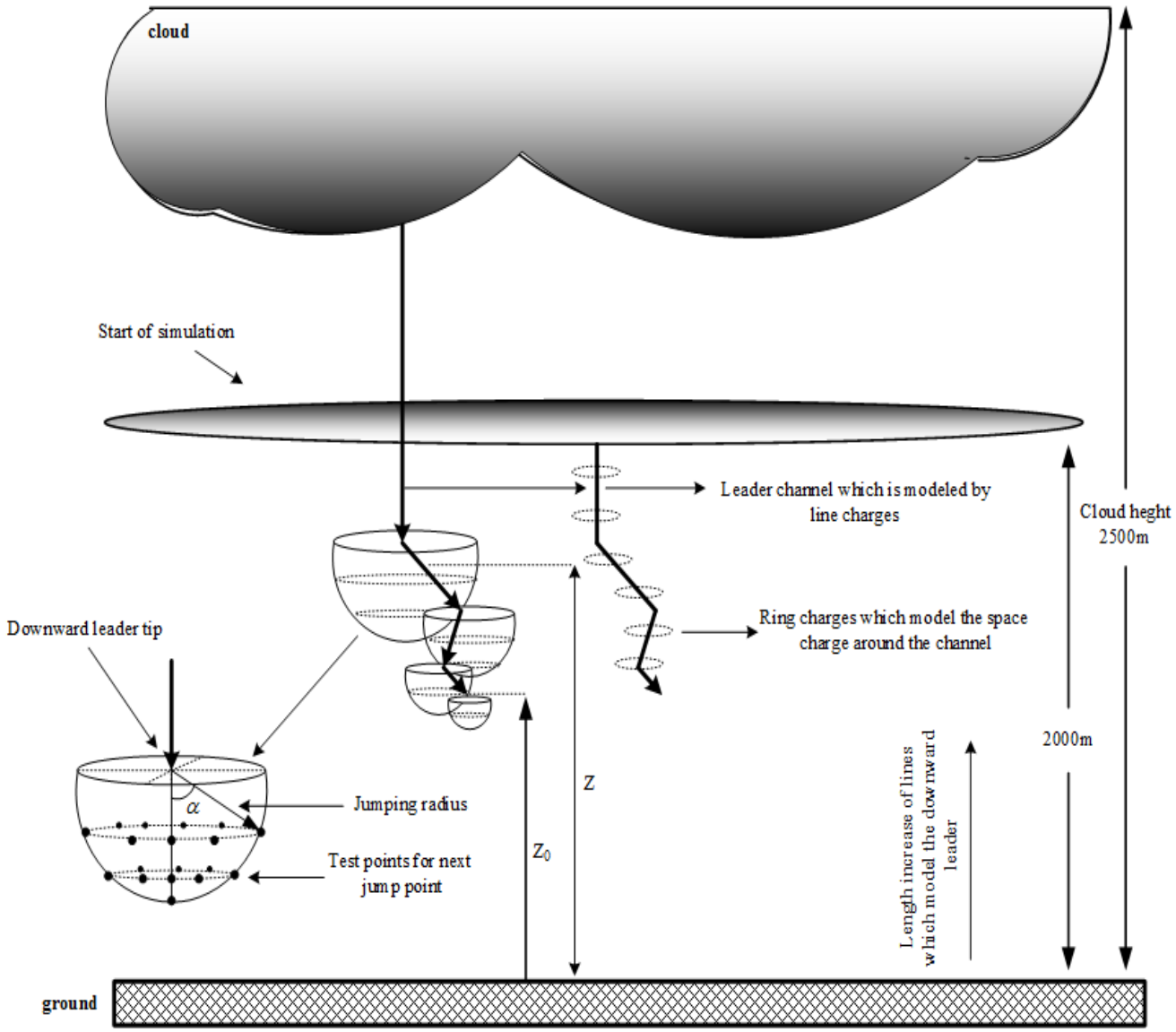

Figure 1. Lightning downward leader modeling.

value of potential is the lowest (i.e., the maximum voltage gradient along the line connecting the leader tip to the target point is ensured)[14]. As the next jump point is determined, the leader moves toward the earth according to determined direction. It should be mentioned that the steps with the length of higher than 100 or lower than 10 meter are estimated to be 100 meter and 10 meter respectively.

After determination of downward leader direction, the charge density of the downward leader must be calculated. There are different equations for computation of charge density and distribution along the leader channel[16,20]. In this paper, the Equation (1) which is proposed[21], is used. This equation calculates the non-linear distribution of charge storing in the lightning stepped

leader channel with high level of accuracy, based on the results of[22], and[23].

$$\rho(z)=I_p\left\{k_0\left(1-\frac{z-z_0}{H_{cloud}-z_0}\right)\left(1-\frac{z_0}{H_{cloud}}\right)+\frac{k_1+k_2(z-z_0)}{1+k_3(z-z_0)+k_4(z-z_0)^2}\left[0.3e^{\frac{10-z_0}{75}}+0.7\left(1-\frac{z_0}{H_{cloud}}\right)\right]\right\} \quad (1)$$

where ρ is the linear charge density of downward leader in (C/m) which is related to Z (i.e., the height of the point on the leader where charge density is to be calculated), Z_0 is the downward leader tip height in (m), I_p is the prospective return stroke peak current in (kA), and H_{cloud} is the height of cloud which is considered to be 2500 meter (based on the field observation of nature[17]. K_0 to K_4 are constant which are presented as follows[21]:

$$k_0=1.476\times10^{-5},\ k_1=4.857\times10^{-5},\ k_2=3.909\times10^{-6}$$
$$k_3=0.522,\ k_4=3.73\times10^{-3} \quad (2)$$

Equation (1) reveals that the charge distribution through the channel is non-linear and the charge variation intensifies in the lower part of the channel. This is in accordance with the nature of downward lightning leader[20]. To take into consideration the mentioned feature of the downward leader in simulation, in this paper, each step of the leader is intersected to unequal segments. The initial and the end point coordinate can be achieved using Equation (3) and Equation (4). The amount of charge of all points in downward leader can be obtained by substituting middle point coordinate (i.e., Equation (5)) in Equation (1). These charges are considered as space charges in CSM calculation.

$$Z_1(k)=-a\times\frac{1-r^{(n-1)}}{1-r}+H_{cloud} \quad (3)$$

$$Z_2(k)=-a\times\frac{1-r^{(n)}}{1-r}+H_{cloud} \quad (4)$$

$$Z_c(k)=\frac{Z_1(k)+Z_2(k)}{2} \quad (5)$$

$$a=L_{tot}\times\frac{(1-r)}{(1-r^{n+1})} \quad (6)$$

In the foregoing equations, $Z_1(k)$, $Z_2(k)$, and $Z_c(k)$ are the high point coordinate, low point coordinate and middle point coordinate of each segment respectively, $L_{tot}=R_L$, and n is the number of segments in each step. Parameter *r* is constant and determined so that the lengths of segments in the lower part of the leader step decrease. Hence, the value of *r* must be lower than 1 (for instance here is 0.8).

The corona sheath around the leader channel which leads to space charge remaining around the leader channel, is another important issue related to lightning downward leader. This space charge causes fluctuation in electric fields in the environment of study and its effect should be investigated. For consideration of space charge, according to Figure1 the charge sheath around the leader channel can be modeled by ring charges with the radius of 0.5 meter. The center of these ring charges is leader channel and the amount of charge in each ring is considered $-40\,\mu c$ [24].

The downward leader continues its propagation until a stable upward connecting leader from the conductors,

towers or ground is incepted. The point of striking is the point that the stable upward leader is incepted. In the next section, the criterion for stable upward leader identification is introduced.

3. Upward Connecting Leader Modeling

As the downward leader approaches the earth, the electric fields on the earthed instruments such as transmission lines, intensifies. When the electrical field on the structures, especially on the sharp points, reaches a critical value, local ionization and corona incept. In the strong electrical field situation, stable upward leader moves towards the negative downward leader. In this paper, in order to determine the strike point, the stable upward corona-leader inception criterion is used.

Different criteria for stable upward leader inception introduced in the literature. Rizk criterion[25], CESL cri-

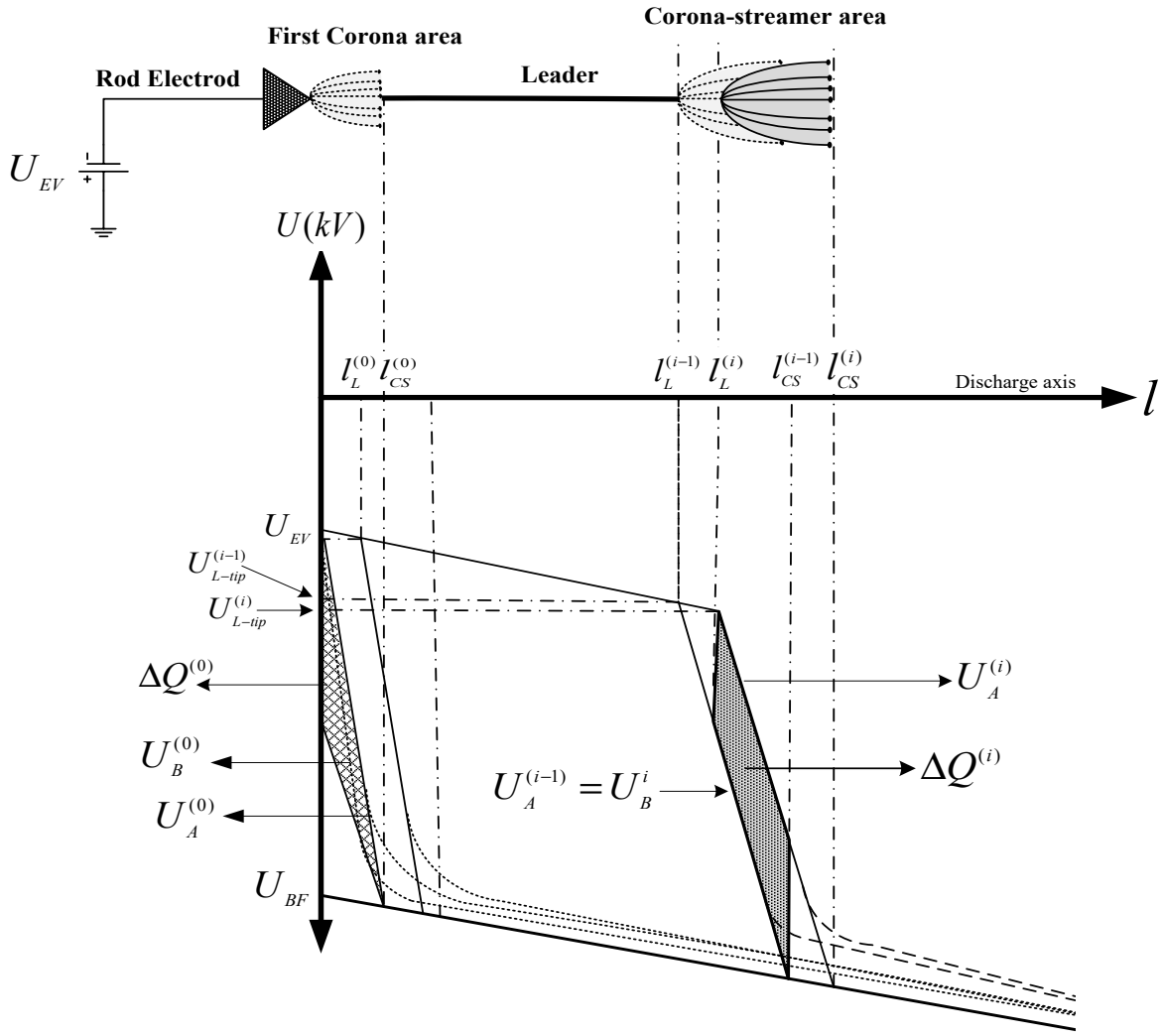

Figure 2. Inception and development of upward corona-leader system and potential distribution of negative electrode.

terion[26], and critical radius criterion[27] are some of the criteria for stable upward leader determination; however, these criteria are appropriate for especial geometric structures. Moreover, the fundamental physical phenomena of upward leader formation are not considered in the mentioned criteria[28]. Recently introduced self-consistent criteria consider the inception of upward leader more accurately[28–30]. These criteria take into consideration the space charge development and transition of the corona streamer to the leader-corona upward connecting system. Nevertheless, computation procedure of lightning modeling based on these criteria is complicated and time consuming. In addition, since these criteria are introduced for earthed electrode, they are unusable for phase conductor with positive and negative voltage. To overcome the issues, in this paper, the self-consistent criteria are improved in such a way that not only the computation procedure became simpler, but also the effect of electrode voltage in stable leader-streamer upward connecting system is considered.

A needle-shaped electrode with negative voltage and its geometric potential distribution in electrical field of downward leader and thunder cloud is depicted in Figure 2 As said before; the formation of stable connecting upward leader is done with the corona-streamer formation and its conversion to corona-leader system in certain circumstances. To implement the self-consistent model, at the zeroth step, the amount of charge in corona zone must be calculated as follows:

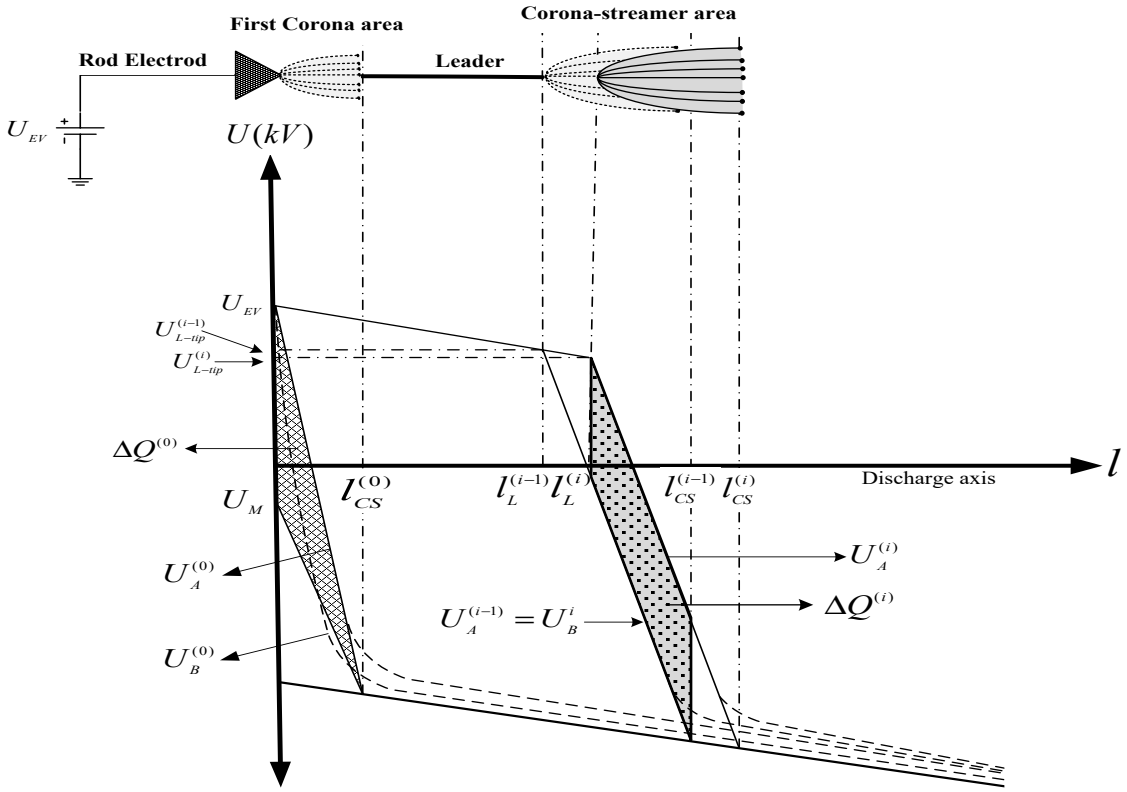

Figure 3. Inception and development of upward corona-leader system and potential distribution of positive electrode.

$$l_{CS}^{0}=\frac{U_{BF}-U_{EV}}{E_{cs}-E_{b}} \tag{7}$$

$$\Delta Q^{0}=\frac{K_{Q}}{2}.\left(\frac{l_{cs}^{0}}{2}\right)^{2}\cdot\left(E_{cs}-E_{b}\right) \tag{8}$$

where U_{BF} is the voltage of fitted line of background electrical field (E_b) as presented in Figure 2 E_{cs} is the corona-streamer zone electrical field which can be considered constant[31], U_{EV} is the electrode potential, l^{0}_{cs} is the length of corona-streamer zone in the zeroth step in front of electrode, and K_Q is the geometric factor which takes into consideration the effect of geometric structure of corona-streamer zone in total amount of charge in this zone. Becerra obtained $K_Q=3.5\times10^{-11}\,C/V.m$ using CSM[29].

The necessary circumstance for conversion of initial corona-streamer to initial unstable corona-leader, is that the amount of charge in this zone must be higher than a critical value (i.e., $\Delta Q^{0}\geq 1\mu c$). In such a situation, an unstable corona-leader system incepts in front of the electrode.

With a similar analysis, the amount of space charge in corona-streamer zone ($\Delta Q^{(i)}$), the development of leader channel ($\Delta l_L^{(i)}$), and the final leader length ($l_L^{(i+1)}$) are calculated in the i[th] step as follows:

$$U_{L-tip}^{(i)}=\left|U_{EV}-\Delta U_{leader}\right| \tag{9}$$

$$U_{L-tip}^{(i)}=\left|U_{EV}-\left(E_{\infty}\cdot L_{L}^{i}+x_{0}\cdot E_{\infty}\cdot\ln\left[\frac{E_{i}}{E_{\infty}}-\frac{E_{i}-E_{\infty}}{E_{\infty}}e^{-L_{L}^{i}/x_{0}}\right]\right)\right| \tag{10}$$

$$\Delta Q^{(i)}\approx K_{Q}\cdot\left(\left(l_{s}^{(i-1)}-l_{L}^{(i)}\right)\cdot\left(\left[E_{str}\left(l_{L}^{(i)}-l_{L}^{(i-1)}\right)+U_{tip}^{(i-1)}-U_{tip}^{(i)}\right]\right)\right) \tag{11}$$

$$\Delta l_{L}^{(i)}=\frac{\Delta Q^{(i)}}{q_{L}} \tag{12}$$

$$l_{L}^{(i+1)}=l_{L}^{(i)}+\Delta l_{L}^{(i)} \tag{13}$$

where $U_{L-tip}^{(i)}$ is the leader tip voltage in i[th] step, ΔU_{leader} is the voltage drop through the leader channel[25], E_{∞} and E_i are initial and ultimate values of the leader gradient respectively[25], $x_{\circ}=v.\theta$ and v is the upward leader velocity, θ is time constant of conductance variation of the leader channel (usually in the range of 30-60 μc [25]), and q_L is the charge per unit length in the situation that the ionization region of corona-streamer can provides the necessary charge for supplying the energy needed for thermodynamic processes of leader expansion[30].

The necessary condition of formation of a upward leader is that in each step $\Delta Q^{(i)}\geq 1\mu c$ [28]. If $\Delta Q^{(i)}<1\mu c$ the simulation procedure is stopped and the upward leader becomes unstable. The simulation procedure continues as long as $l_L^{(i)}=l_{\max}$. In this paper, $l_{\max}$ is considered the half value of distance between downward leader tip and target point.

The formation process of stable upward corona-leader system from positive or earthed electrode can be stated according to that of negative electrode. The formations of stable upward leader for positive electrode are exhibited

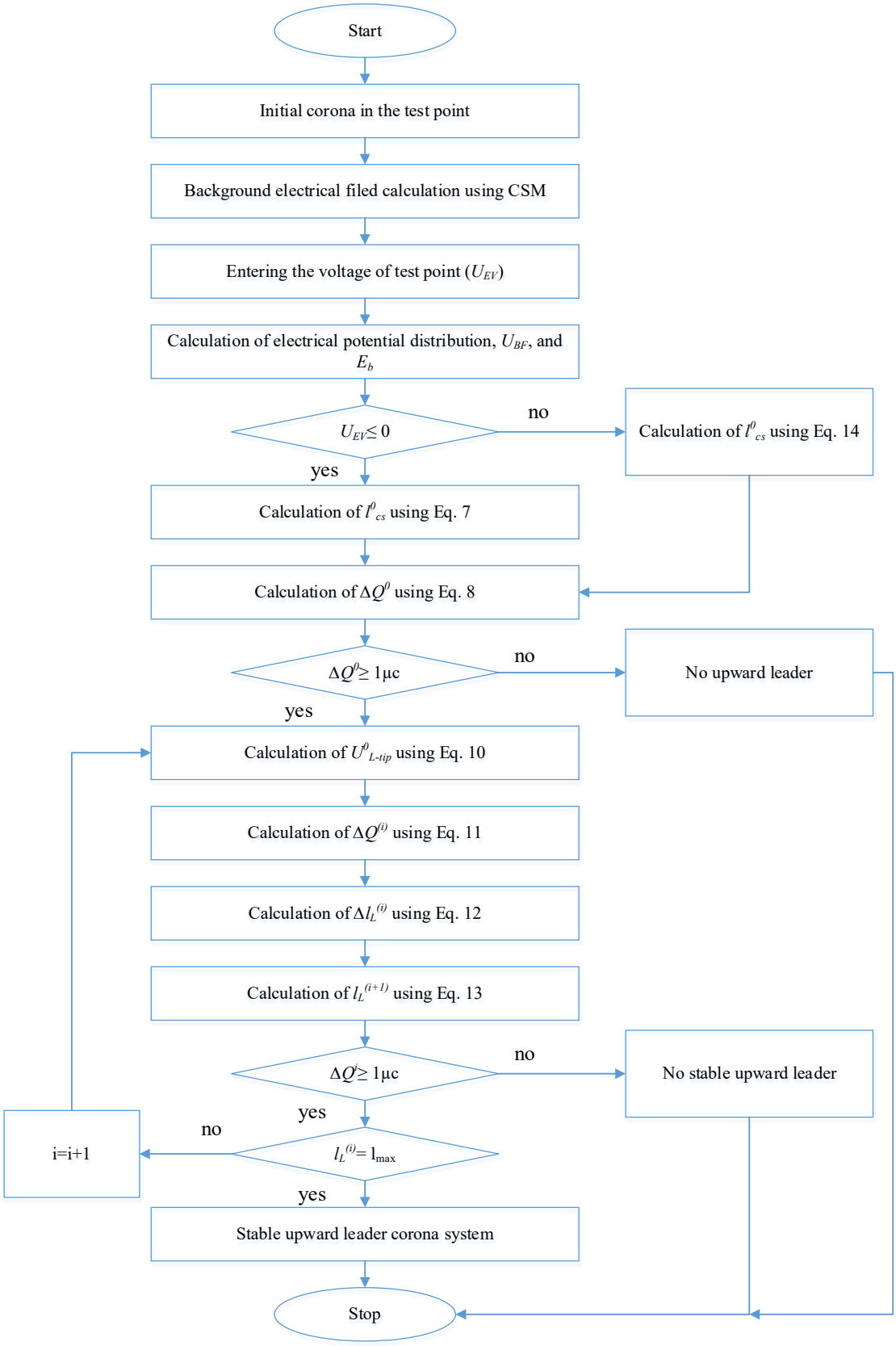

Figure 4. Flowchart of checking the stable upward leader formation.

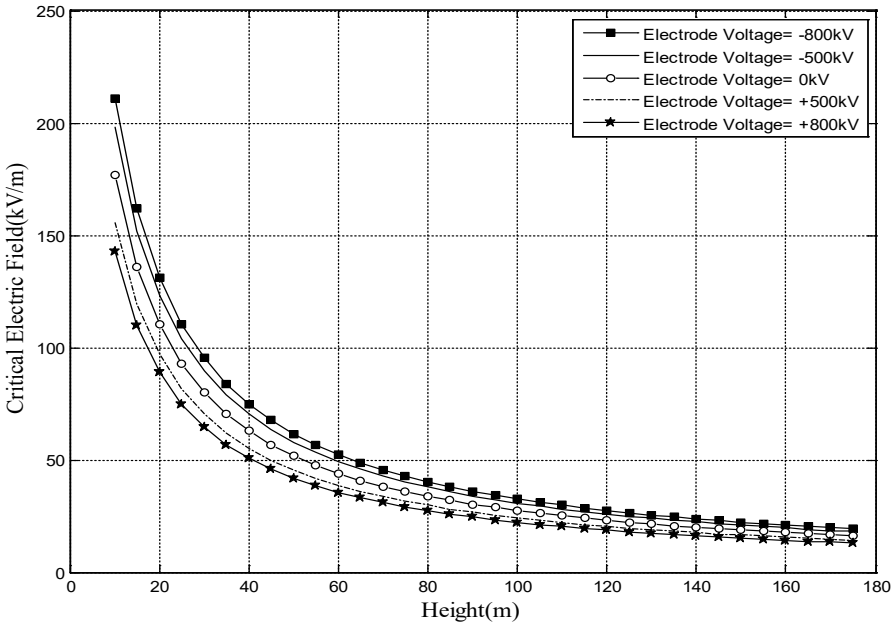

Figure 5. Electrical field of stable upward corona-leader for rod-shaped electrode in different voltage levels.

in Figure 3, 4. All equations and computational processes outlined in the negative electrode can be applied for upward corona-leader from positive electrode. Just Equation (7) changes to Equation (14).

$$l_{CS}^{0} = \frac{U_{BF} + U_{EV}}{E_{cs} - E_{b}} \tag{14}$$

The computational processes for earthed electrode are completely the same with negative electrode, just the voltage is considered as zero.

Figure 4 shows the flowchart of checking the stable upward leader formation.

Eelectrode with the curvature radius of 1cm in different voltage level is depicted in Figure 5. The constant parameters used for upward leader modeling is listed in Table 1.

Based on the Figure 5 as the negative downward leader approaches to the electrode, the critical field required for the inception of stable upward leader varies with the variation of magnitude and the sign of electrode voltage. This critical field for the positive voltage of electrode is much lower than the cases of zero or negative voltage. The difference of critical field is increased as the electrode voltage level increases. The simulation results are coincident with the field experiments[32]. They concluded that the stable upward leader inception from the +800kV conductor is far faster than the conductors with +500kV and zero voltage level. Based on these phrases, it can be concluded that the probability of lightning strokes to the phase wire with positive voltage is much higher than that of phase wires with zero voltage or negative voltage. These conclusions are confident with field experiments on ±500kV HVDC transmission line in Tian-Guang and Gui-Guang in

Table 1. Different parameters of upward positive leader-corona system for calculation of SFR

Parameter	Description	Value	Unit	Ref
E_{cs}	Corona-Streamer zone constant electric field	450	kV/m	[31]
K_Q	geometrical factor that takes into accountthe effect of all of the streamers on the total charge	3.5×10^{-11}	$C/V.m$	[29]
E_∞	Ultimate values of the leader gradient	30	kV/m	[34]
E_i	Initial values of the leader gradient	450	kV/m	[31]
v	Upward leader velocity	15000	m/s	[25]
θ	Conductance variation time constant of upward leader	50	μs	[25]
q_L	charge per-unit length necessary to achieve the thermal transition from the diffuse glowto the leader channel	65	C/m	[30]

china[32]. The monitoring of foregoing HVDC transmission lines in 2003-2006 shows 8 outages from which 7 outages occurred in positive voltage conductor and just one of them occurred in negative voltage conductor. Therefore, it is so important to consider the voltage level and sign of conductor in striking point determination and lightning return stroke current.

4. Simulation of Space of Study

In this section, the modeling of transmission lines, towers and cloud in the environment of study are illustrated. The modeling is based on virtual charges which are explained in details in[13,14].

4.1 Cloud Modelling

The clouds are modeled as virtual negative ring charge in the height of the clouds. There are ring charges for each cloud with the center of mid-span of transmission line and expansion of 5000m. It should be mentioned that the earth effect is considered by the image charge with the opposite sign. After determination of the virtual charge location, the amount of these charges in the storm condition is determined using boundary conditions. The electric field on the objects surface is in the range of 1-20 kV/m in the storm condition[17]. Therefore, the cloud virtual ring charges are determined so that in each step of downward leader, the electric field near the ground becomes 10kV/m.

4.2 Tower Modelling

Due to the symmetrical and cylindrical structure of the towers, ring charges are used for modeling of towers[14]. The number of ring charges is selected so that the error of

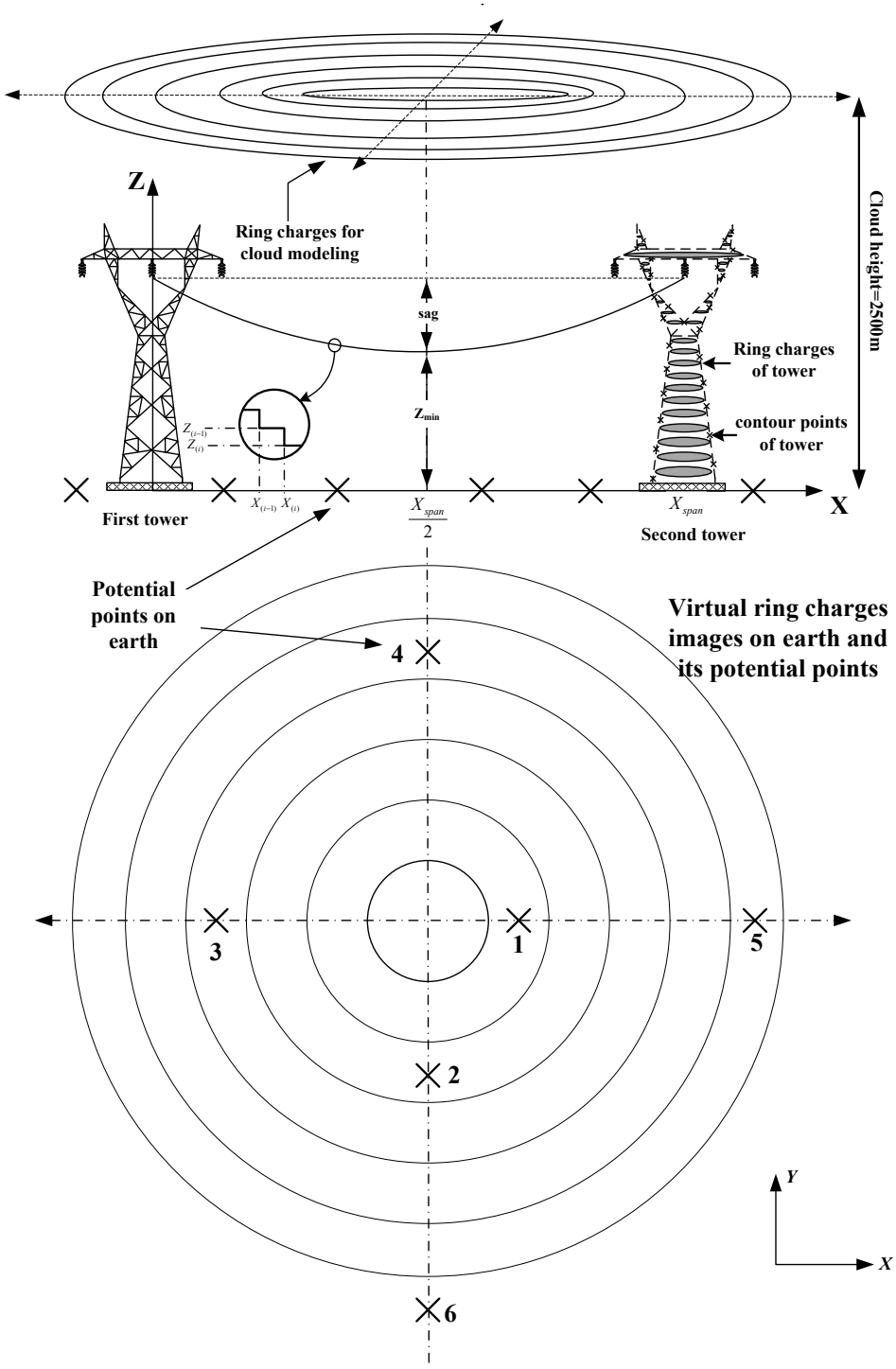

Figure 6. Cloud and tower modeling based on ring charges, and phase conductor and shield wires modeling using vertical/horizontal line charges.

calculated potential on the surface of tower (which must be zero) is minimized. The simulations revealed that 26 ring charges for each tower is appropriate. Consideration of more ring charges increases the time and volume of calculations; while, does not have a significant effect on the accuracy of the calculations. Thus, in this paper, 26 rings are considered for each tower with the radius based on tower structure. The rings are placed in different parts of towers such as cross arms. Zero voltage is considered as boundary condition for determination of virtual charges. Figure 6 presents the ring charges and contour points location.

4.3 Conductors Modelling

In this paper, for the modeling of phase conductors and shield wires, vertical/horizontal line charges are used[14]. In order to considering the sag of wires, hyperbolic equation is used. The equation for each point of wire (x_i, y_i) is as follow:

$$z_i = Z_{\min} \times \cosh(m \times (x_i - \frac{X_{span}}{2})) \quad (15)$$

where:

$$m = \frac{2}{X_{span}} \times \cosh^{-1}(\frac{Z_{phase}}{Z_{\min}}) \quad (16)$$

As it can be seen in Figure 6, Z_{phase} is the height of wires in the point of connection to tower and X_{span} in the span length of transmission line.

The instantaneous voltage of phase conductor and zero voltage of shield wires are considered as boundary conditions. The manner of consideration of sinusoidal behavior of phase conductor voltage in HVAC transmission line is illustrated later.

5. SFR Calculation Of High Voltage Transmission Lines

Figure 7 exhibits the space of study in which there are a transmission line span and the ground. According to Figure 7 for SFR calculation, a rectangular area for the inception of downward leader is considered. Length of this area is considered equal to length of span and width of area is considered large enough so that, out of the area no flash occurs to the wires and towers. To cover all points of the area, the area is dived into meshes with the length of $dx = (1/20) \times span$ and width of $dy = 10m$. In each step of simulation procedure, a downward leader is incepted from the center of each mesh. The downward leader approaches to the earth according to Section 2, and the strike point is determined using stable upward leader inception criteria. To reduce the computation procedure, due to symmetrical structure of span, only $1/2$ of rectangular area is considered. It should be mentioned that because of consideration of phase conductor voltage, unlike the references[13,14], the span is not symmetric in Y direction.

To cover all lightning which strikes to the transmission line, simulation procedure for each mesh is performed for a reasonable range of lightning current. In this paper, the range of lightning current is considered between 1kA to 50kA with the step of 0.3kA.

The simulation procedure is started with a vertical 500m leader which is incepted from point (x_i, y_i) in the height of 2500m. The leader movement is simulated step by step. In each step, the virtual charges are placed in different locations and the electrical field and potential are calculated in the space of study. By the calculation of electrical field, the stable upward leader condition in all test points on the wires and tower are checked. If the

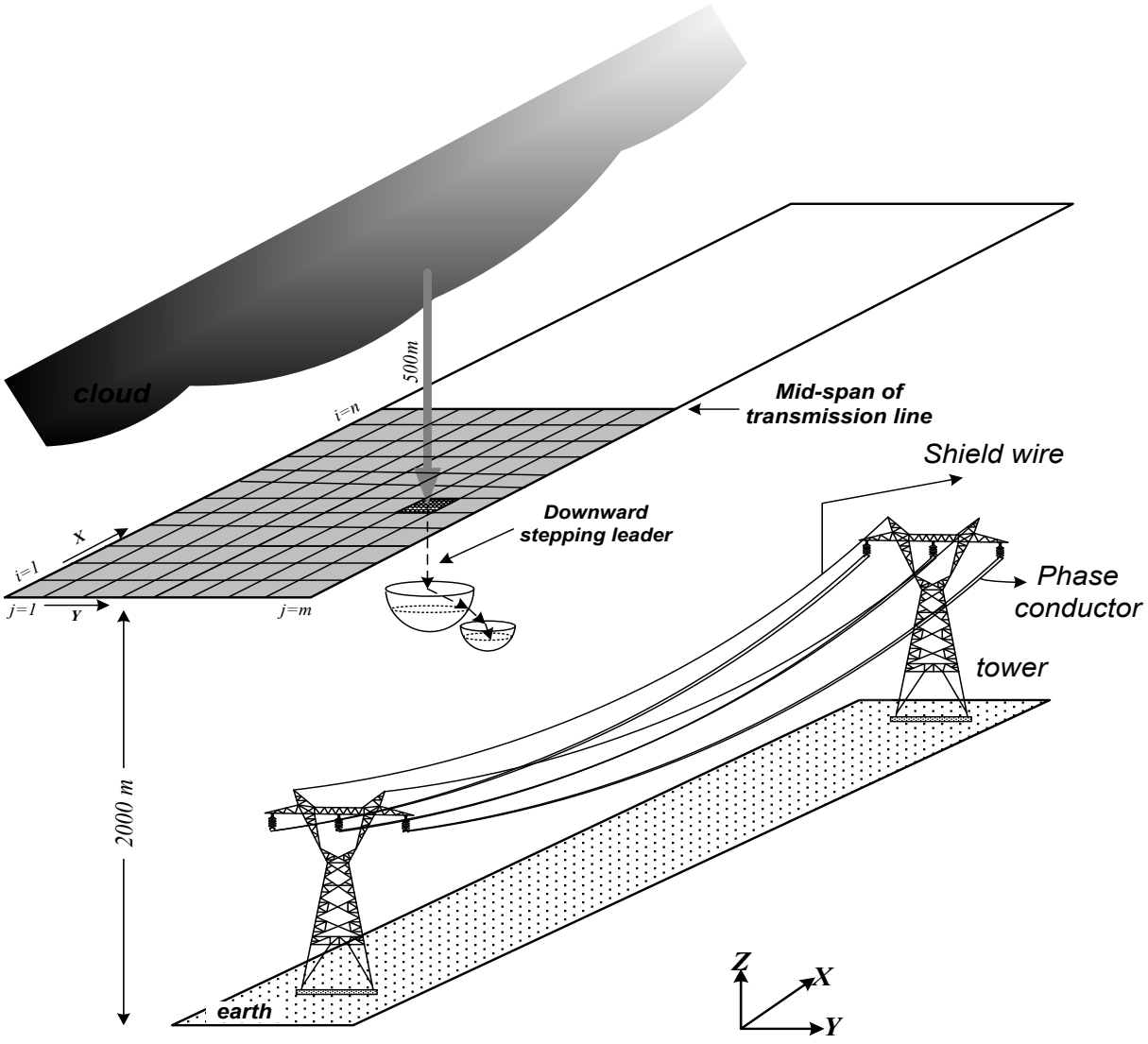

Figure 7. 3-D modeling of simulation space for SFR calculation of transmission line.

conditions causing the stable upward leader in each of these test points, the simulation ends. The model used for stable upward leader inception is the model which is introduced in section III with the consideration of voltage effect. It should be noticed that if the stable upward leader incepts from more than one point, the strike point will be the point which the upward leader connects to downward leader in fewer steps. Moreover, the lightning strikes to the ground, if there are no stable upward leader from the test points while the downward leader reaches to the height of 5 meter.

After consideration of all meshes and lightning currents, the range of lightning current which causes striking to the phase conductor is determined as $(I_{min}, I_{max})_{(i,j)}$.

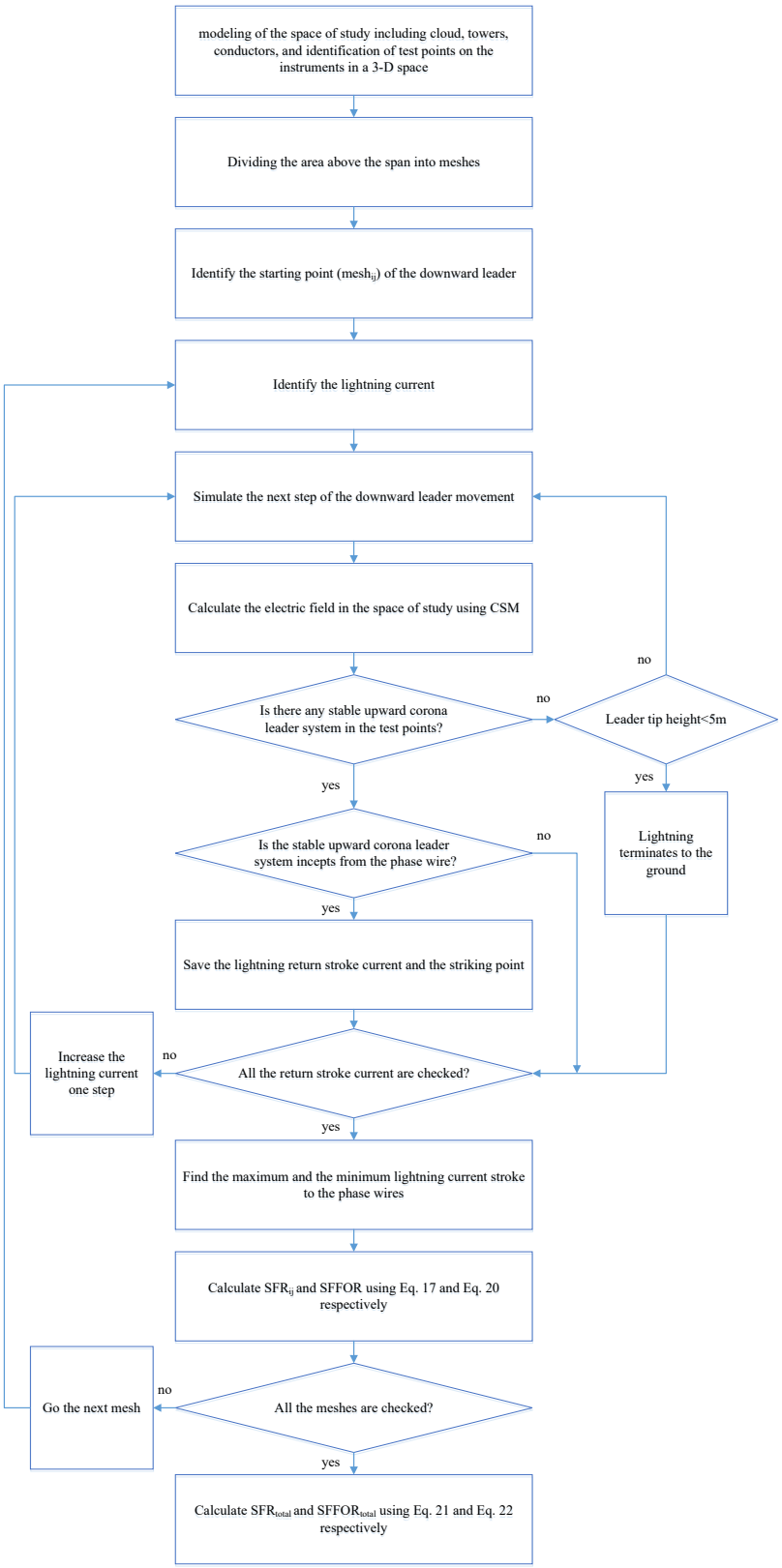

Figure 8. The procedure for calculating the SFR and SFFOR of transmission lines with the proposed method.

Then after, the SFR for the mentioned situation (i.e., SFR_{ij}) is calculated.

$$SFR_{ij} = 0.1 \times GFD \times \frac{dx.dy}{X_{span}} \int_{I_{min}}^{I_{max}} P(I)dI \quad (17)$$

where SFR_{ij} is the shielding failure rate in strokes/100km-year of mesh(x,y), GFD is the ground flash density in strokes per square kilometers per year and can be calculated as $GFD = 0.015 \times T$ [16],T_d is the isokeraunic level which is equal to 40, P(I) is the probability of lightning current to be more than I and calculated as follow[16]:

$$P(I_P \geq I) = 10^{(0.05 - \frac{I}{74})} \quad (18)$$

dx and dy are the length and width of mesh in meter respectively, and X_{span} is the length of transmission line span in meter.

Shielding failures with low lightning Stroke currents may not necessarily cause flashover on transmission lines. Therefore, I_c is considered as the critical current which causes flashover as follow:

$$I_c = \frac{2(CFO + U_{transient})}{Z_S} \quad (19)$$

where CFO (kV) is the critical lightning impulse flashover voltage of the insulation, Z_s (Ω) is the conductor surge impedance under corona and $U_{transient}$ is the instantaneous operating voltage of the transmission line in kV. Now, SFFOR can be calculated as follow:

$$SFFOR_{ij} = 0.1 \times GFD \times \frac{dx.dy}{X_{span}} \int_{I_C}^{I_{max}} P(I)dI \quad (20)$$

The total SFR and SFFOR for the transmission line is the summation of SFR_{ij} and $SFFOR_{ij}$ for all meshes as follow:

$$SFR = 2 \times \sum_{j=1}^{m} \sum_{i=1}^{n} SFR_{ij} \quad (21)$$

$$SFFOR = 2 \times \sum_{j=1}^{m} \sum_{i=1}^{n} SFFOR_{ij} \quad (22)$$

Figure 8 shows the procedure for calculating the Shielding Failure of transmission lines with the proposed method.

For consideration of sinusoidal behavior of phase voltage in HVAC transmission line, the period of center phase voltage is divided into 12 equal angular intervals (i.e., $\omega t = 0°, 30°,$). The voltage of center phase is calculated for these different phases. The voltage of outside phases can be obtained considering 120° phase difference. Considering these voltages as boundary condition, the SFR and SFFOR are calculated. This procedure is performed for all voltage angles. The SFR and SFFOR of transmission line are the average of SFR and SFFOR during a sinusoidal voltage period.

6. Simulation and Results

A 500kV-HVAC transmission line in China is considered as the case study. In order to compare the results, the selected structure is the same with structure in[14–16]. Therefore, tower dimensions and the transmission line information are illustrated in detail in[14].

As explained in the previous sections, for SFR calculation of HVAC transmission line considering the sinusoidal behavior of phase voltage, a period is divided into different angles and the SFR is calculated for all discrete parts. Total SFR is the mean of all SFR values. Figure 9 exhibits the SFR (upper part) and the maximum return stroke current (lower part) in different angles of

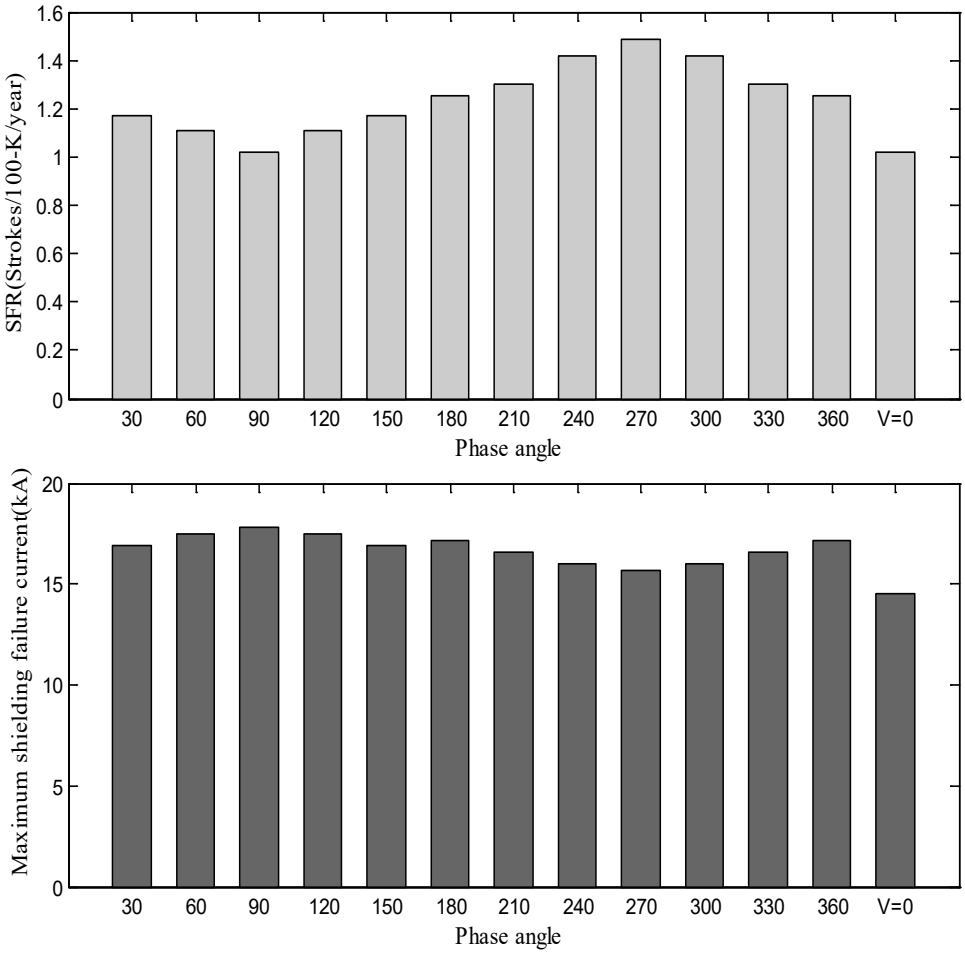

Figure 9. SFR and maximum return stroke current in different voltage angles of 500kV-HVAC transmission line.

AC voltage. It should be mentioned that the center phase is considered in calculation procedure and the 120° different phase must be considered for outside phases. The results are compared with the cases in which the effect of the voltage is neglected and the comparison is shown in Figure 9.

As it can be seen in Figure 9 the SFR and maximum return stroke current are changed with the variation of phase voltage angle. The maximum SFR is occurred in the angle of 270° where the center phase voltage is in its maximum negative value and the outside phases voltage are +0.5 of positive peak voltage. On the other side, the minimum SFR is occurred when the center phase voltage is in the maximum positive value. Moreover, the values of SFR in the angles that the outside phases voltages are positive are higher than those where the outside phases voltages are negative.

This relation between SFR and phase angle variation can be justified based on Section 3. When the phase angle changes during a period, the value of voltage varies. In the half of period where the voltage is positive, the needed electrical field for upward leader inception

Table 2. The SFR and maximum return stroke current for 500kV-HVAC transmission line with and without consideration of phase voltage

	SFR(Strokes/100km-year)	Maximum return stroke current (kA)
With consideration of phase voltage	1.2508	16.8
Without consideration of phase voltage	1.0182	14.5

is lower in comparison to that when the voltage is negative. Therefore, positive upward leader incepts from the conductor with positive voltage faster in comparison to conductor with negative or zero voltage level.

It should be mentioned that the results obtained by the proposed approach are coincident with the field measurements in[33,34]. They investigate the effect of phase variation of operating voltage on the upward leader inception for a

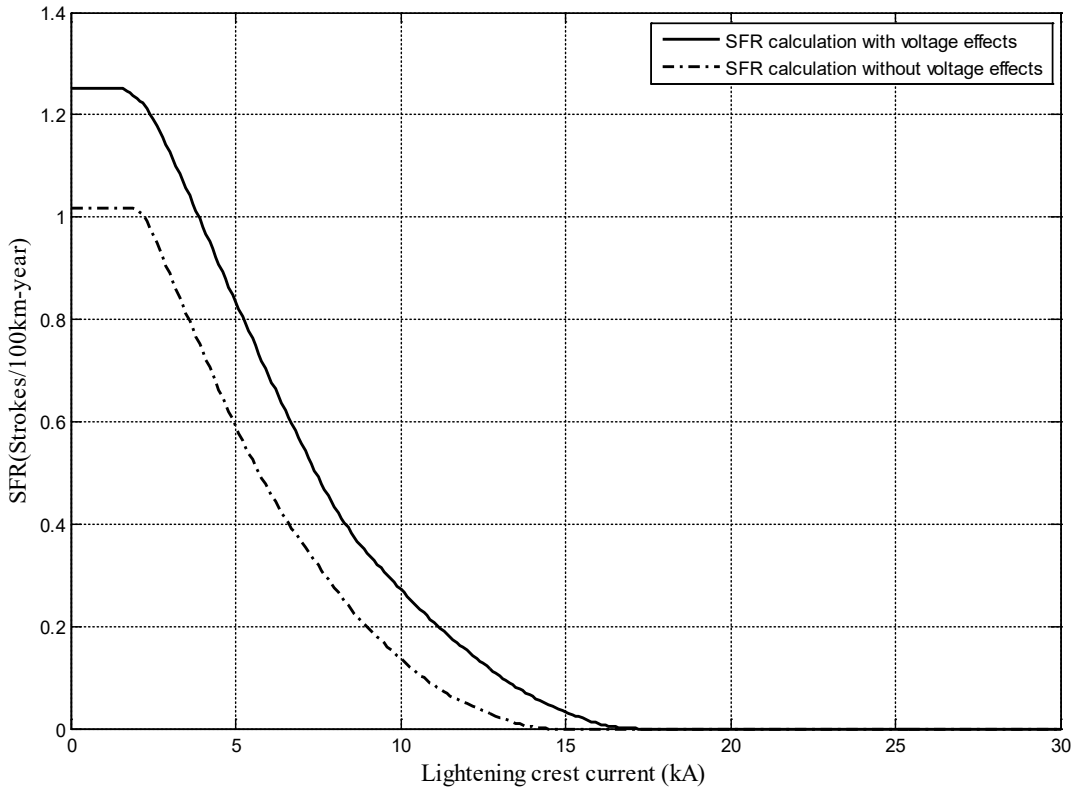

Figure 10. Comparison of SFR of 500kV-HVAC transmission line with and without consideration of phase voltage.

Table 3. The comparison of SFR and maximum return stroke current obtained in this paper and other published articles in an equal transmission line structure

Method	SFR (Strokes/Km-year)	Maximum Return Stroke Current(kA)	Percentage of different with LPM model (SFR/Imax)
Proposed Method	1.2508	16.8	-/-
[16]	5.5	19.2	339/14
Rizk Criterion[14]	1.01	14.8	19/12
Macroscopic Criterion[14]	1.81	16.2	45/3.5
EGM[16]	0.548	11.4	56/32

500 kV-HVAC transmission line. They concluded that as the magnitude of the voltage increases (with variation of voltage phase), the upward leader incepts faster.

The calculated SFR based on LPM model and consideration of phase voltage of 500kV-HVAC transmission line is depicted and compared to SFR without voltage consideration in Figure 10. As it can be seen,consideration of voltage of phase conductor results in increase in SFR.

In Figure 10 the horizontal axis refers to lower bound of integration in Equation 20 i.e., I_c. Thus, SFFOR can be calculated for different values of critical current (I_c). The overall SFR is the junction point between the Figure and the vertical axis. On the other side, the maximum return stroke is the junction point between the Figure and horizontal axis. The values are listed in Table 2.

It can be comprehended from the Table 2 that the SFR and maximum return stroke current increase 19% and 14% respectively by consideration of phase voltage. Therefore, for a more accurate calculation of SFR, consideration of phase voltage is vital. The effect of phase voltage is taken into consideration for all further calculations.

The calculated SFR of this paper is compared to the results of EGM[16], numerical analyses model[16], and CSM model$_{14}$ in Table 3. The structure of studied transmission line in all three papers is the same. The thunderstorm days is considered 40 days in a year and the probability density function of lightning is calculated by Equation (18).

As the Table 3 shows, the maximum SFR is obtained by the method introduced in[16], and the minimum SFR is calculated using EGM. The results of[14] with Rizk criterion are the closest to the results of this paper.

In Table 4 the result of SFR obtained by the proposed approach is compared to that of improved LPM[15]. Here, T_d=40 and GFD=2.9 flash/km^2.year. The probability density function of lightning current, based on the China's standard, is calculated as follow:

Table 4. The comparison of SFR and maximum return stroke current obtained in this paper and Improved LPM

Method	SFR (Strokes/Km-year)	Maximum Return Stroke Current(kA)	Percentage of different with Proposed Method (SFR/Imax)
Proposed Method	0.2465	16.8	-/-
Improved LPM[15]	0.2135	10.3	15/63

$$P(I)=\frac{\ln 10}{88}10^{(-\frac{I}{88})} \quad (23)$$

As it can be seen, the SFR and Maximum Return Stroke Current (kA) obtained by the proposed approach are 15% and 63%, respectively, higher than those obtained by the improved LPM in[15]. These differences will be discussed in the next section.

7. Discussion

In this section the reason of differences between the results of this paper and the results of other methods and also the superiority of the proposed approach are explained briefly.

In EGM model the strike point is determined based on striking distance and the stepping procedure of lightning downward leader is not simulated. Moreover, the electrical field of downward leader movement and the upward leader inception are not taken into consideration. While, in this paper, the process of lightning movement between the cloud and the earth is simulated accurately in 3-D space.

In[16], and the improved LPM[15], the downward leader path is considered vertically; while, the field observations reveal that the downward movement of lightning has tortuosity. The zigzag movement of downward leader, in this paper, is simulated using horizontal and vertical finite line charges. Furthermore, the tower of transmission lines are simulated by means of ring charges to consider the strokes to the tower and also the effect of tower charges on the electric field distortion. It should be mentioned that the EGM[16], and improved LPM[15], neglect the lightning strokes to the tower and the tower effects on the background electric field distribution. Moreover, in this paper, the sag of conductor is modeled using vertical and horizontal finite line charges; while the effect of conductor sag is neglected in EGM[16], and improved LPM[15].

In[14] the Rizk criterion and macroscopic criterion are considered as upward leader inception criteria. In[15], the Rizk criterion and Carrara criterion[27] are used for stable upward leader identification from shield wires and phase wires, respectively. These criteria are considered for the conductor with zero voltage level. Application of these criteria for the phase wire with sinusoidal voltage may decrease the accuracy of calculations. The phrase is demonstrated in the field experiments[32].

In this paper, the effect of operating voltage (magnitude and sign of voltage) is considered in striking point and lightning characteristics determination (using the model illustrated in Section 3). Moreover, the effect of sinusoidal behavior of operating voltage is investigated in

both the striking point determination and SF calculation; while, in[14], only the positive peak of the voltage is considered as the worst case. This consideration may results in inaccurate calculation. It should be mentioned that although the sinusoidal voltage is considered in SFFOR calculation in[15], there is no explanation about the effect of sinusoidal nature of voltage on initial corona formation and its conversion to a stable upward leader system.

8. Conclusion

SFR calculation of high voltage transmission line is performed using Leader Progression Model. In this paper, unlike the previous attempts of SFR calculation, the effect of operating voltage (including the magnitude, sign, and the sinusoidal nature of voltage) is considered in upward leader inception process, striking point identification, and return stroke current magnitude. For this purpose, a criterion for stable upward leader identification considering the operating voltage is developed. The results based on the proposed criterion showed that the probabilities of upward leader inception and lightning strokes vary with variation of voltage operating of conductors. In the conductor with positive voltage, the required electric field for upward leader inception is far lower than the conductors with zero or negative voltage. This difference increases as the voltage magnitude increases.

In this paper, the sinusoidal behavior of phase voltage is taken into consideration in SFR calculation. From the results it was comprehended that neglecting the alternative voltage of phase conductor results in lower SFR. Moreover, the phase difference of three phase voltage, affect the SFR of transmission line. For instance, the results show that the highest and lowest value of SFR occurs in the phase of 270° and 90°of center phase voltage, respectively, where the side phases voltages are in the half positive peak value (+0.5V), and the middle phase voltage is in negative peak value.

The method introduced in this paper is applied for investigation of shielding performance of a 500-kV HVAV transmission line in china. The results reveal that the SFR and maximum return stroke current increase 19% and 14% respectively by consideration of phase voltage.

Finally, the amount of SFR of this paper with consideration of voltage effect and its sinusoidal behavior, compared to the results of other researchers and the differences are investigated. It can be said that the results of this paper is more accurate compared to previous attempts because of consideration of operating voltage and its sinusoidal nature, accurate simulation of downward leader and its transition charge and detail modeling of space of study.

9. References

1. Hileman AR. Insulation coordination for power systems. CRC Chain Reaction Cycles Press. 1999 Jun; 19(9):1–43. Crossref.
2. Young FS, Clayton JM, Hileman AR. Shielding of transmission lines. IEEE Transactions on Power Apparatus and Systems. 1963 Apr; 82(4):132–54.
3. Anderson JG. Lightning performance of transmission lines. Transmission Line Reference Book, 345 kV and Above; 1981. p. 1–74.
4. Armstrong HR, Whitehead ER. Field and analytical studies of transmission line shielding. IEEE Transactions on Power Apparatus and Systems. 1968 Jan; 87(1):270–81. Crossref.
5. Brown GW, Whitehead ER. Field and analytical studies of transmission line shielding: Part. IEEE Transactions on Power Apparatus and Systems. 1969 May; 88(5):617–26. Crossref.
6. Golde RH. The frequency of occurrence and the distribution of lightning flash to transmission lines. Electrical Engineering. 1945 Dec; 64(12):902–10. Crossref.
7. Love ER. Improvements in lightning stroke modeling and applications to the design of EHV and UHF transmission

lines. [Doctoral dissertation, University of Colorado]; 1973. p. 1–14.

8. Suzuki T, Miyake K, Shindo T. Discharge path model in model test of lightning strokes to tall mast. IEEE Transactions on Power Apparatus and Systems. 1981 Jul; 100(7):3553–62. Crossref.
9. Whitehead JT, Chisholm WA, Anderson JG, Clayton R, Elahi H, Eriksson AJ, Grzybowski S, Hileman AR, Janischewskyj W, Longo VJ, Moser CH. Estimating lightning performance of transmission line 2-Updates to analytical models. IEEE Transactions on Power Delivery. 1993 Jul; 8(3):1254–67. Crossref.
10. Rizk FA. Modeling of transmission line exposure to direct lightning strokes. IEEE Transactions on Power Delivery. 1990 Oct; 5(4):1983–97. Crossref.
11. Dellera L, Garbagnati E. Lightning stroke simulation by means of the leader progression model. II. Exposure and shielding failure evaluation of overhead lines with assessment of application graphs. IEEE Transactions on Power Delivery. 1990 Oct; 5(4):2023–9. Crossref.
12. Sima W, Li Y, Rakov VA, Yang Q, Yuan T, Yang M. An analytical method for estimation of lightning performance of transmission lines based on a leader progression model. IEEE Transactions on Electromagnetic Compatibility. 2014 Dec; 56(6):1530–9. Crossref.
13. Tavakoli MR, Vahidi B. Transmission-lines shielding failure-rate calculation by means of 3-D leader progression models. IEEE Transactions on Power Delivery. 2011 Apr; 26(2):507–16. Crossref.
14. Vahidi B, Yahyaabadi M, Tavakoli MR, Ahadi SM. Leader progression analysis model for shielding failure computation by using the charge simulation method. IEEE Transactions on Power Delivery. 2008 Oct; 23(4):2201–6. Crossref.
15. Wei B, Fu Z, Yuan H. Analysis of lightning shielding failure for 500-kV overhead transmission lines based on an improved leader progression model. IEEE Transactions on Power Delivery. 2009 Jul; 24(3):1433–40. Crossref.
16. He J, Tu Y, Zeng R, Lee JB, Chang SH, Guan Z. Numeral analysis model for shielding failure of transmission line under lightning stroke. IEEE Transactions on Power Delivery. 2005 Apr; 20(2):815–22. Crossref.
17. Bazelyan EM, Raizer YP. Lightning physics and lightning protection. CRC Press; 2000. Crossref.
18. Malik NH. A review of the charge simulation method and its applications. IEEE Transactions on Electrical Insulation. 1989 Feb; 24(1):3–20. Crossref.
19. Singer H, Steinbigler H, Weiss P. A charge simulation method for the calculation of high voltage fields. IEEE Transactions on Power Apparatus and Systems. 1974 Sep; 93(5):1660–8. Crossref.
20. Cooray V. The mechanism of the lightning flash. The Lightning Flash. 2003, 34, pp. 1-127. Crossref.
21. Cooray V, Rakov V, Theethayi N. The lightning striking distance- Revisited. Journal of Electrostatics. 2007 May; 65(5):296–306. Crossref.
22. Berger K. Methods and results of lightning records at Monte San Salvatore from 1963–1971. Bull. Schweiz. Elektrotech. ver. 1972, 63, pp. 21403-22.
23. Berger K. Measurement and results of lightning records at Monte San Salvatore from 1955-1963. Bull. Schweiz Elektrotech. 1965; 56:2–2.
24. Willett JC, Davis DA, Laroche P. An experimental study of positive leaders initiating rocket-triggered lightning. Atmospheric Research. 1999 Jul; 51(3):189–219. Crossref.
25. Rizk FA. Switching impulse strength of air insulation: Leader inception criterion. IEEE Transactions on Power Delivery. 1989 Oct; 4(4):2187–95. Crossref.
26. Kumar U, Bokka PK, Padhi J. A macroscopic inception criterion for the upward leaders of natural lightning. IEEE transactions on power delivery. 2005 Apr; 20(2):904–11. Crossref.
27. Carrara G, Thione L. Switching surge strength of large air gaps: a physical approach. IEEE Transactions on Power Apparatus and Systems. 1976 Mar; 95(2):512–24. Crossref.
28. Goelian N, Lalande P, Bondiou-Clergerie A, Bacchiega GL, Gazzani A, Gallimberti I. A simplified model for the simulation of positive-spark development in long air

gaps. Journal of Physics D: Applied Physics. 1997 Sep; 30(17):1–2441. Crossref.

29. Becerra M, Cooray V. A simplified physical model to determine the lightning upward connecting leader inception. IEEE Transactions on Power Delivery. 2006 Apr; 21(2):897–908. Crossref.
30. Lalande P, Bondiou-Clergerie A, Bacchiega G, Gallimberti I. Observations and modeling of lightning leaders. ComptesRendus Physique. 2002 Dec; 3(10):1375–92. Crossref.
31. Gallimberti I. The mechanism of the long spark formation. Le Journal de Physique Colloques. 1979 Jul; 40(C7):1–193. Crossref.
32. Zeng R, Li Z, Yu Z, Zhuang C, He J. Study on the influence of the DC voltage on the upward leader emerging from a transmission line. IEEE Transactions on Power Delivery. 2013 Jul; 28(3):1674–81. Crossref.
33. Wang X, Yu Z, He J, Zeng R. Characteristics of upward leader emerging from a single-phase conductor with different voltage class. IEEE Transactions on Power Delivery. 2015 Aug; 30(4):1833–42. Crossref.
34. Rizk FA. Modeling of lightning incidence to tall structures. I. Theory. IEEE Transactions on Power Delivery. 1994 Jan; 9(1):162–71. Crossref.